



X線非弾性散乱研究における将来展望

—XFELへの期待—

原子力機構放射光

石井賢司

Outline

- ◇ Non-resonant Inelastic X-ray Scattering (NIXS)
 - Electronic excitation
 - Phonon excitation
 - (X-ray Raman Scattering, core-level excitations)

- ◇ Resonant Inelastic X-ray Scattering (RIXS)
 - Electronic excitation

- Introduction

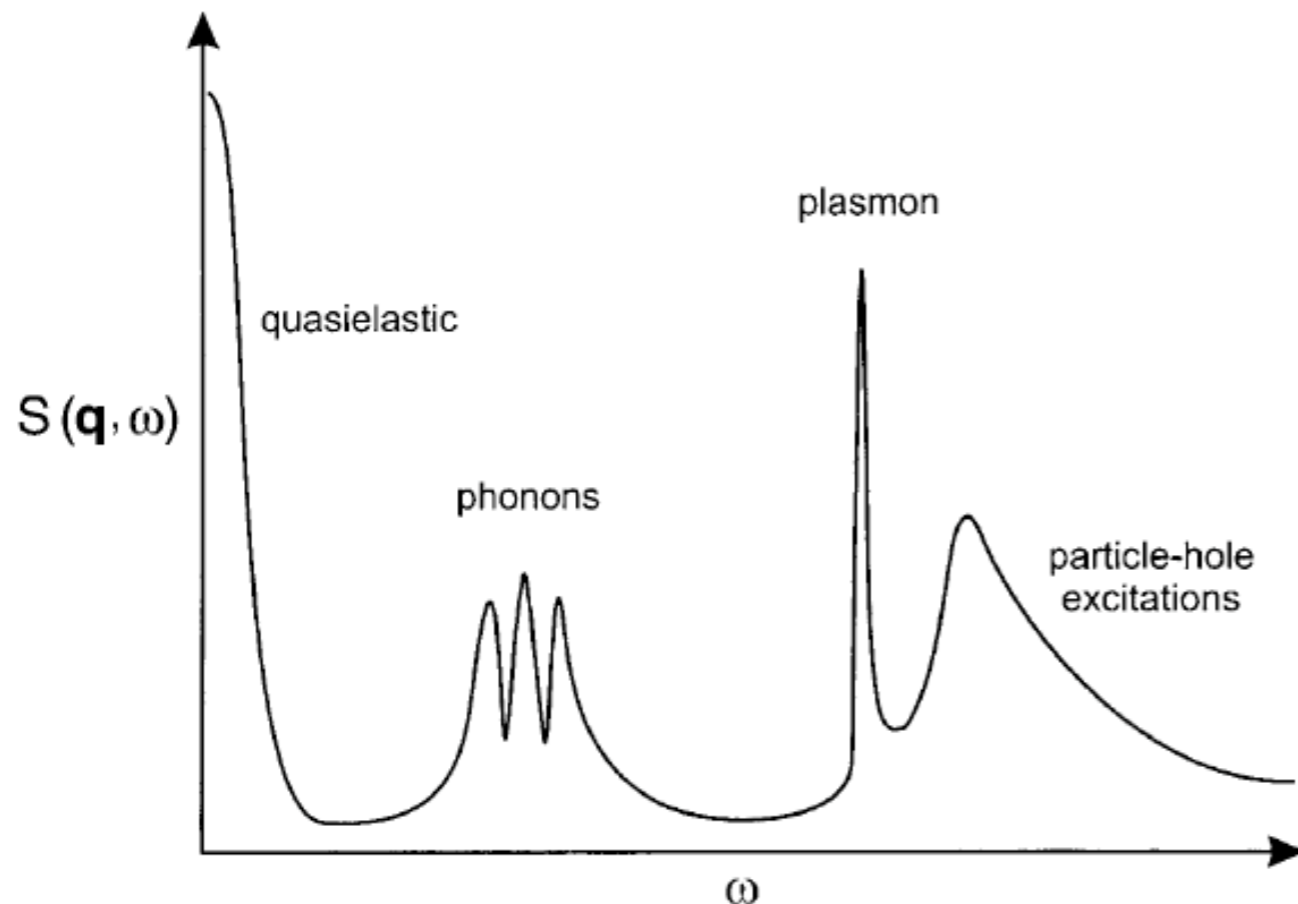
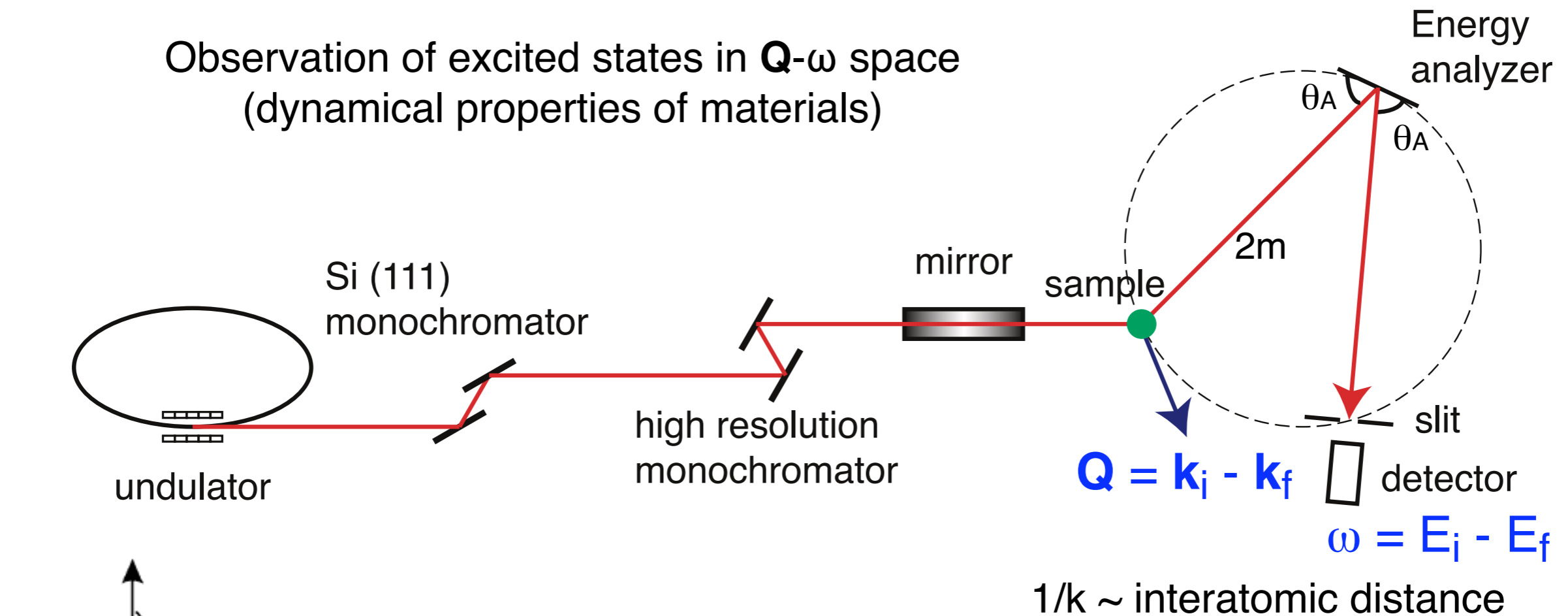
- History and current topics

- XFEL as an x-ray source of IXS

- Scientific cases

Inelastic x-ray scattering

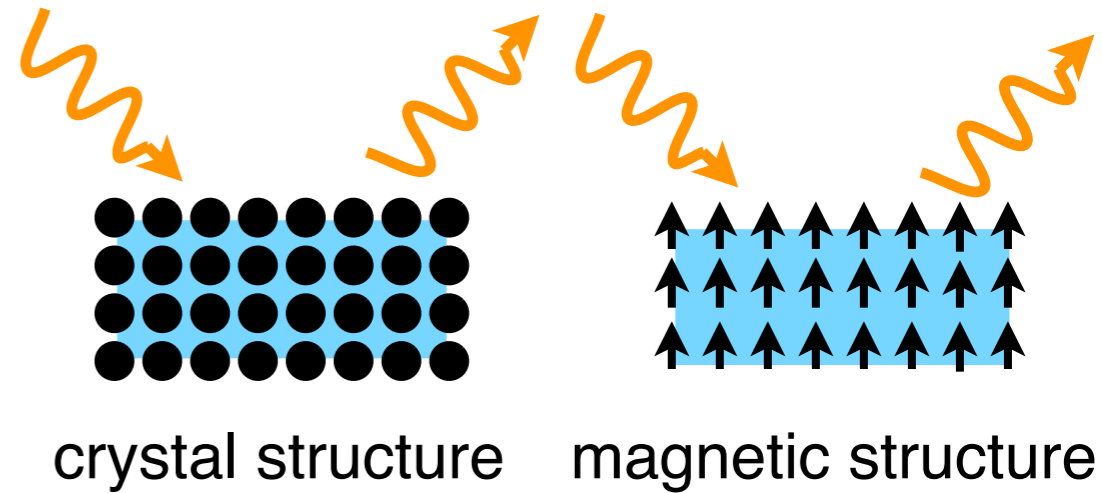
Observation of excited states in \mathbf{Q} - ω space
(dynamical properties of materials)



What can we learn by inelastic scattering ?

1. **static properties [ground state]**
 identification of ordered state

photon
 neutron
 electron



elastic scattering (diffraction)

2. **dynamical properties [excited state]**

- elementary excitation
 → underlying interaction of electrons
 understanding of mechanism

- fluctuation

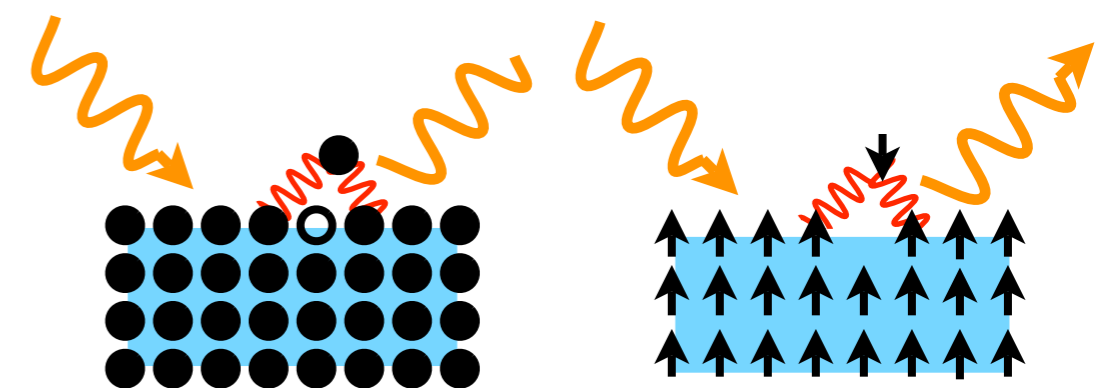
$$S(\mathbf{Q}, \omega) \sim [V(\mathbf{Q})]^2 [1 - e^{-\beta\omega}]^{-1} \text{Im}\chi(\mathbf{Q}, \omega)$$

$S(\mathbf{Q}, \omega)$: dynamical correlation function

$V(\mathbf{Q})$: interaction of probe

$\chi(\mathbf{Q}, \omega)$: response function (susceptibility)

- response to external field
 function of materials



charge

band gap, width

Coulomb repulsion

spin

exchange (J)

inelastic scattering

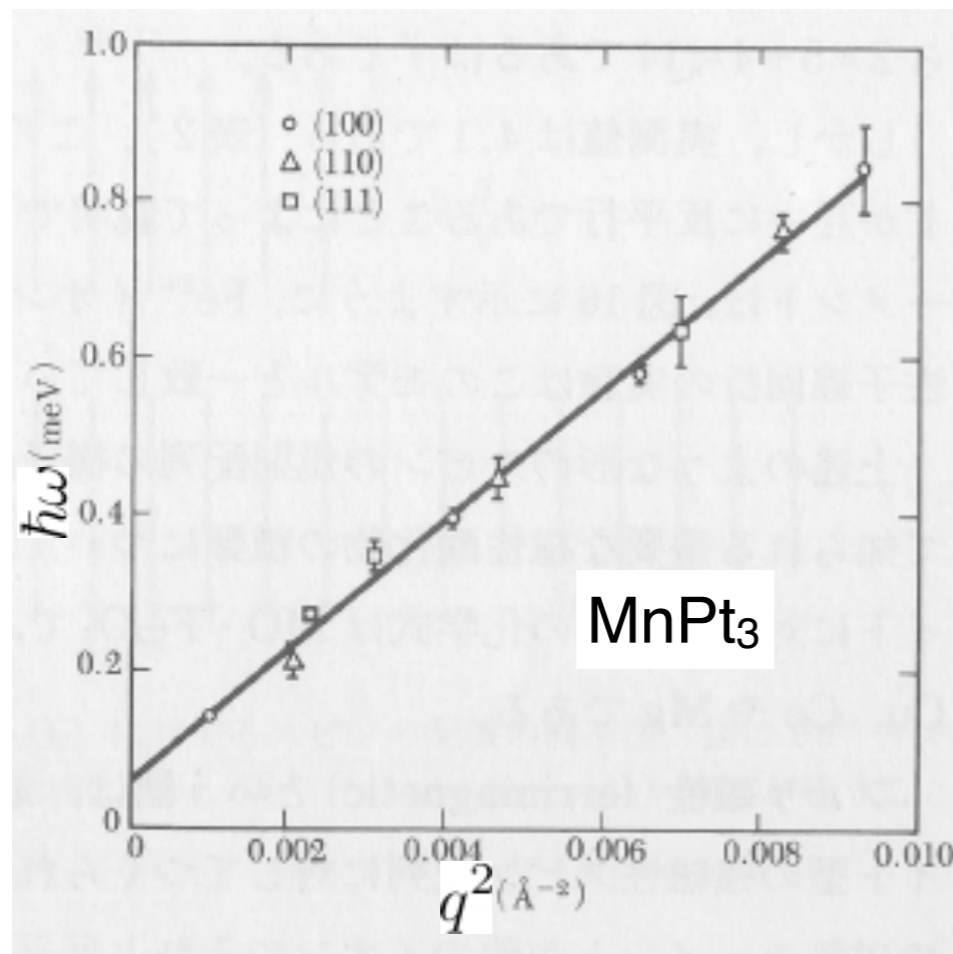
Inelastic magnetic scattering from magnetic order

magnetic excitation (spin wave)

ferromagnetic order

$$H = -2J \sum_i \mathbf{S}_i \cdot \mathbf{S}_{i+1}$$

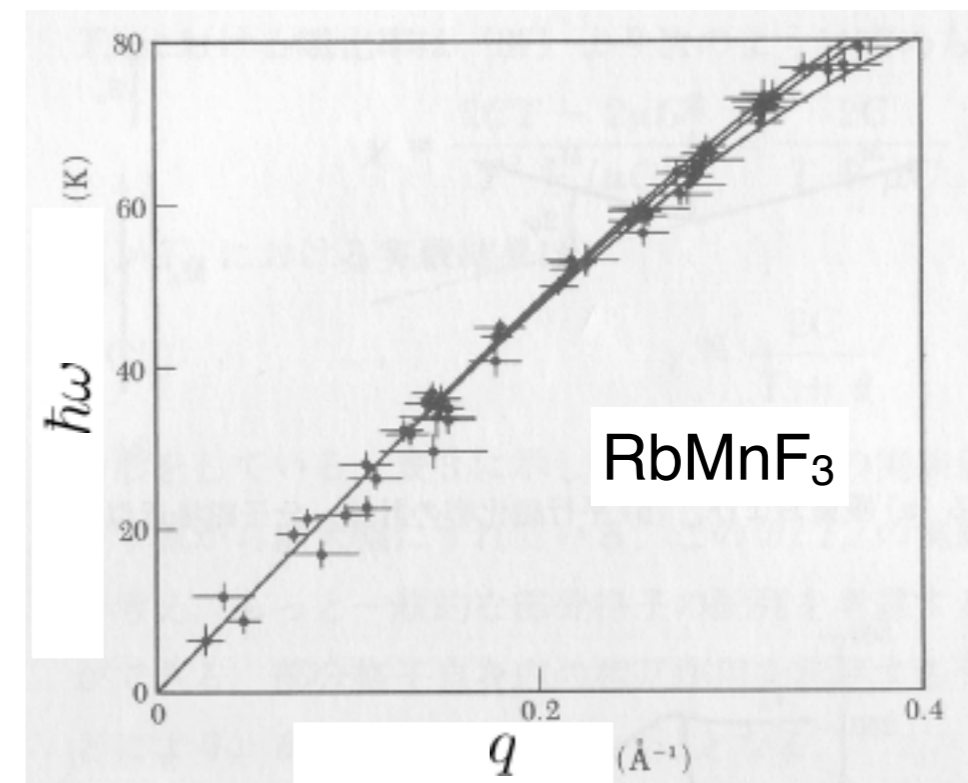
$$E = 4JS(1 - \cos qa) \sim (2JSa^2)q^2$$



antiferromagnetic order

$$H = 2J \sum_i \mathbf{S}_i \cdot \mathbf{S}_{i+1}$$

$$E = 4JS|\sin qa| \sim 4JSa|q|$$



C. Kittel, Introduction of Solid State Physics

dispersion relation of magnetic excitation
 \Rightarrow magnetic interaction J

Non-resonant and resonant x-ray scattering

X-ray interaction with electrons

$$H = \sum_i \frac{1}{2m} \left(\mathbf{p}_i - \frac{e}{c} \mathbf{A}_i(\mathbf{r}_i) \right)^2 + \sum_{ij} V(r_{ij})$$

$$H_0 = \sum_i \frac{\mathbf{p}_i^2}{2m} + \sum_{ij} V(r_{ij})$$

$$H' = -\frac{e}{mc} \sum_i \mathbf{A}(\mathbf{r}_i) \cdot \mathbf{p}_i + \frac{e^2}{2mc^2} \sum_i \mathbf{A}(\mathbf{r}_i)^2$$

1st order of \mathbf{A}^2 term
non-resonant IXS

2nd order of $\mathbf{A} \cdot \mathbf{p}$ term
(Kramers-Heisenberg formula)
resonant IXS

Fermi's golden rule

$$w = \frac{2\pi}{\hbar} \left| \langle f | H' | i \rangle + \sum_n \frac{\langle f | H' | m \rangle \langle m | H' | i \rangle}{E_i - E_m + \hbar\omega} \right|^2 \delta(E_i + \hbar\omega_i - E_f - \hbar\omega_f)$$

$$\left(\frac{d^2\sigma}{d\Omega dE} \right)_{a,\mathbf{k}\lambda \rightarrow b,\mathbf{k}'\lambda} = \left(\frac{e^2}{mc^2} \right)^2 \left| \underbrace{\langle b | \sum_i e^{i(\mathbf{k}-\mathbf{k}') \cdot \mathbf{r}_i} | a \rangle (\boldsymbol{\varepsilon}' \cdot \boldsymbol{\varepsilon})}_{\text{non-resonant}} + \underbrace{\frac{\hbar}{m} \sum_{c,ij} \frac{\langle b | \boldsymbol{\varepsilon}' \cdot \mathbf{p}_i e^{i\mathbf{k}' \cdot \mathbf{r}_i} | c \rangle \langle c | \boldsymbol{\varepsilon} \cdot \mathbf{p}_j e^{-i\mathbf{k} \cdot \mathbf{r}_j} | a \rangle}{E_a - E_c + \hbar\omega_k + i\Gamma_c/2}}_{\text{resonant}} \right|^2 \delta(E_a + \hbar\omega_k - E_b - \hbar\omega_{k'})$$

non-resonant
 $\sim Z^2$

resonant

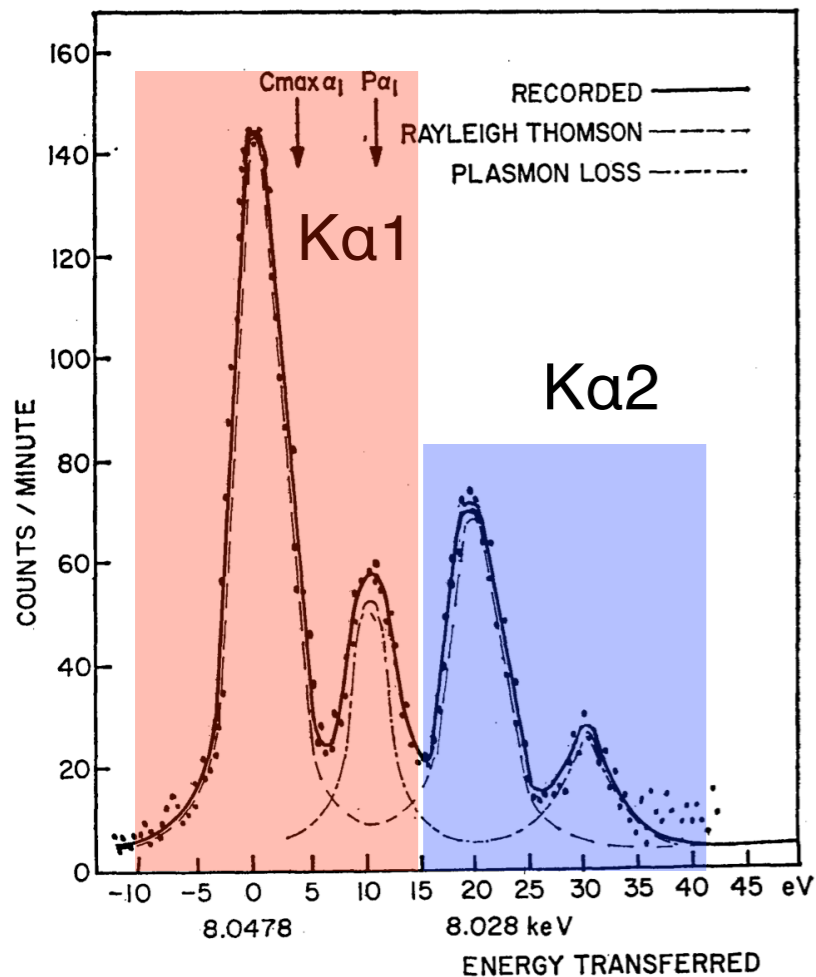
Blume, J. Appl. Phys. **57**, 3615 (1985)

Two types of IXS

Non resonant IXS (NIXS)	Resonant IXS (RIXS)
1st order of A^2 term	2nd order of $A \cdot p$ term
photon energy is far from absorption edge	photon energy is tuned near absorption edge
dynamical charge correlation function $N(Q, \omega) \sim \text{Im}\chi(Q, \omega)$ \Rightarrow simple interpretation	2nd order optical process (complex) excitation by strong core-hole potential qualitative similarity to $N(Q, \omega)$
all electrons contribute evenly	element selective
good energy resolution $\Delta E \sim$ sub meV	poor energy resolution $\Delta E \sim 100$ meV
valence electron excitation across E_F is usually very weak \rightarrow limited to low Z materials phonon excitation (all electron in atom)	resonance enhancement of valence electron excitation
simple polarization dependence	polarization analysis \rightarrow determination of symmetry

NIXS (Electronic excitations)

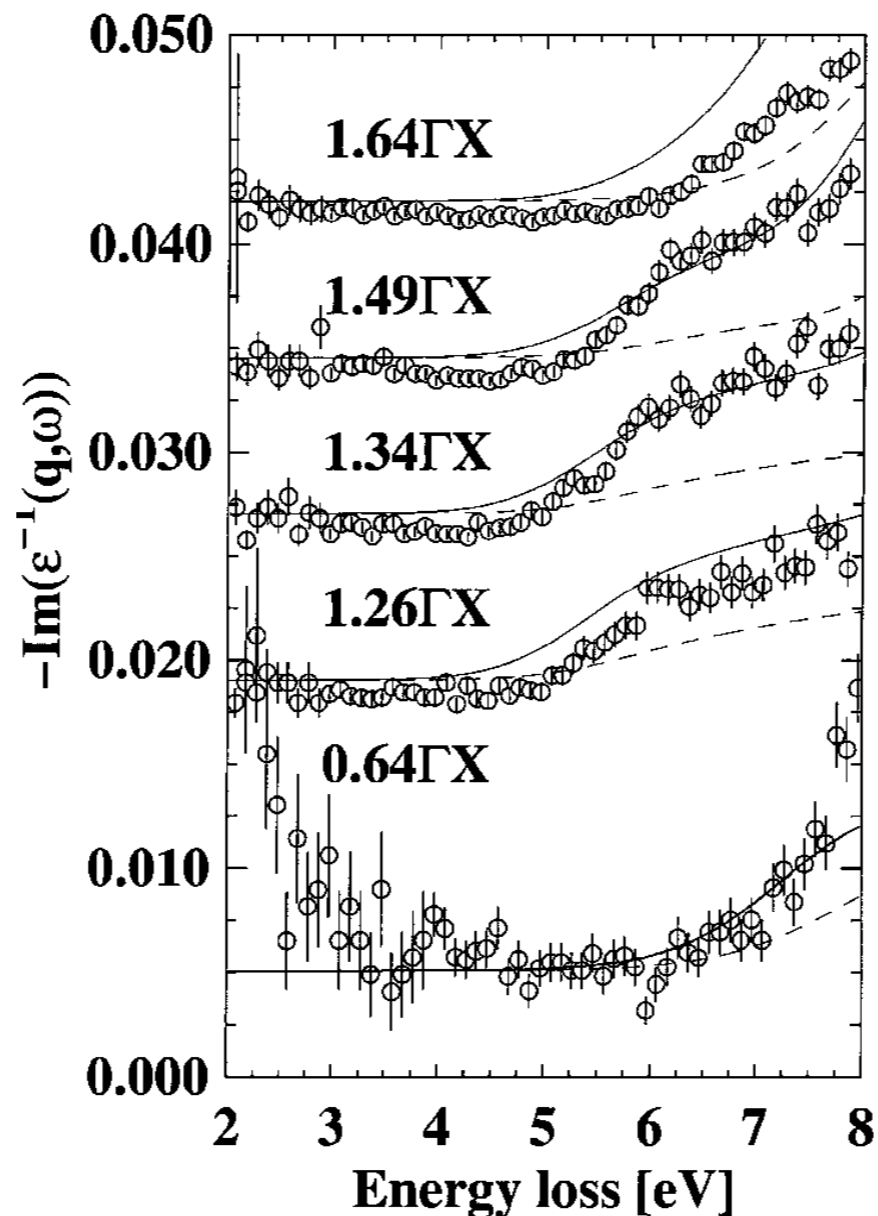
1971
 $\omega = 10 \text{ eV}$



plasmon of Li
(conventional x-ray source)

Alexandropoulos,
JPSJ **31**, 1790 (1971).

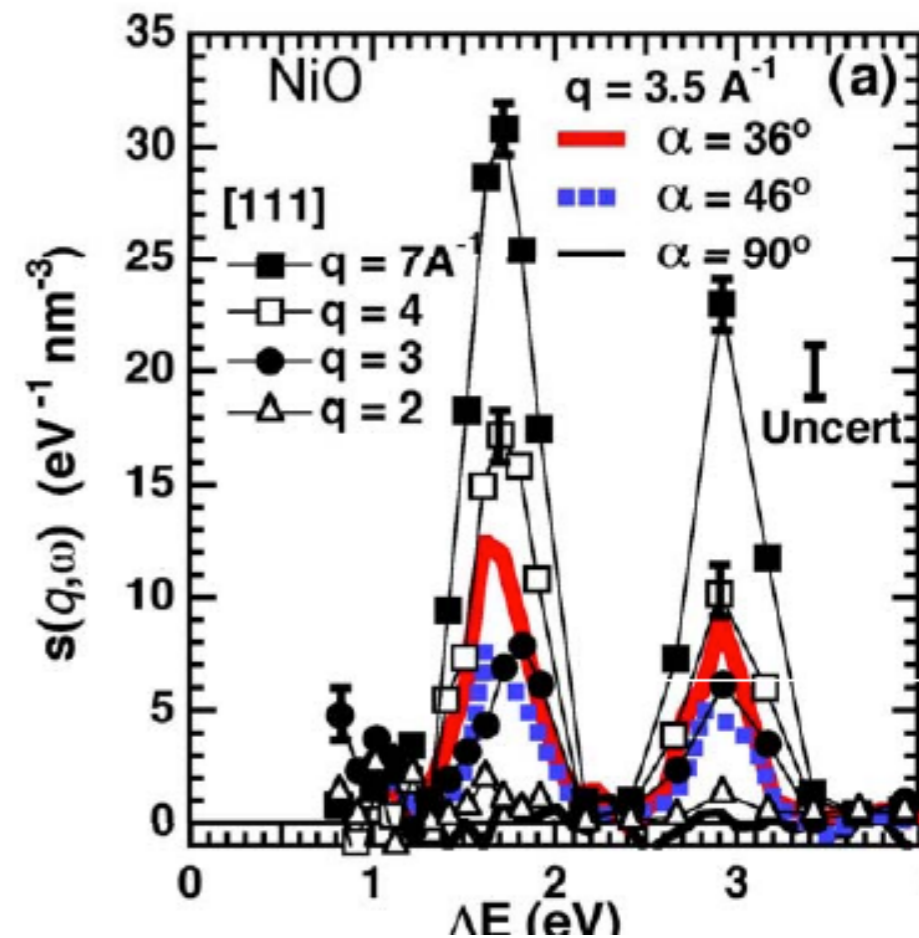
2000
 $\omega = 5 \text{ eV}$



indirect band gap of diamond
(NSLS)

Caliebe et al.,
PRL **84**, 3907 (2000).

2007
 $\omega = 1-2 \text{ eV}$



d-d excitations of NiO
(APS)

Larson et al.,
PRL **99**, 026401 (2007).

Imaging of atomic and attosecond resolution

VOLUME 92, NUMBER 23

PHYSICAL REVIEW LETTERS

week ending
11 JUNE 2004

Imaging Density Disturbances in Water with a 41.3-Attosecond Time Resolution

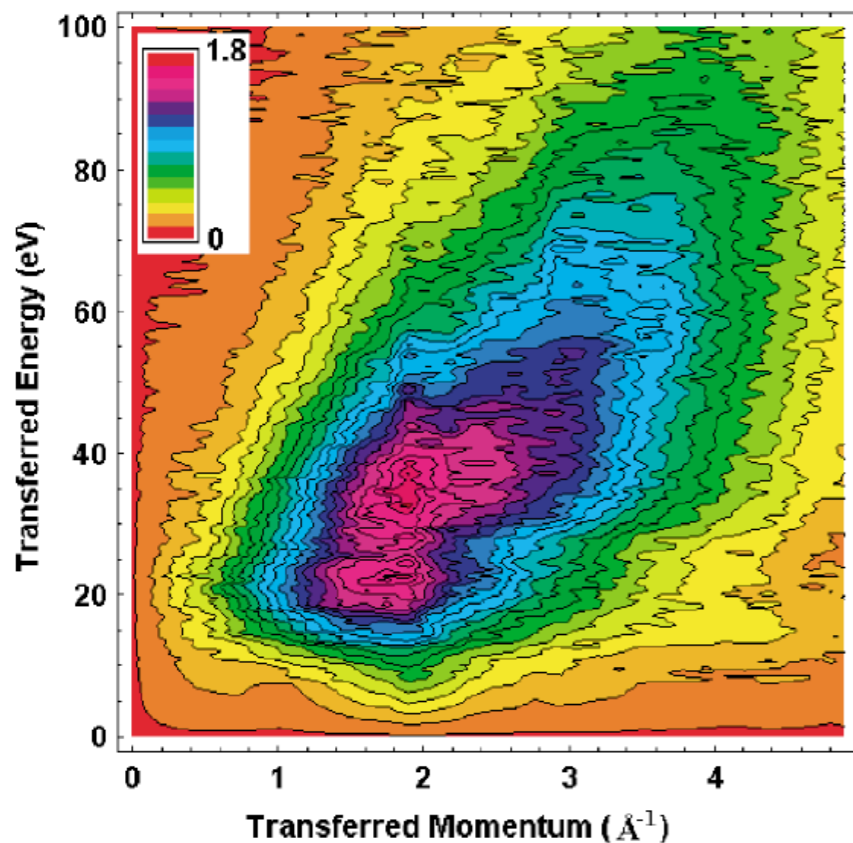
P. Abbamonte,^{1,*} K. D. Finkelstein,² M. D. Collins,¹ and S. M. Gruner^{1,2}

¹*Department of Physics, Cornell University, Ithaca, New York 14853-2501, USA*

²*Cornell High Energy Synchrotron Source, Cornell University, Ithaca, New York 14853-2501, USA*

(Received 15 November 2003; published 11 June 2004)

We show that the momentum flexibility of inelastic x-ray scattering may be exploited to invert its loss function, allowing real time imaging of density disturbances in a medium. We show the disturbance arising from a point source in liquid water, with a resolution of 41.3 attoseconds (4.13×10^{-17} s) and 1.27 Å (1.27×10^{-8} cm). This result is used to determine the structure of the electron cloud around a photoexcited chromophore in solution, as well as the wake generated in water by a 9 MeV gold ion. We draw an analogy with pump-probe techniques and suggest that energy-loss scattering may be applied more generally to the study of attosecond phenomena.



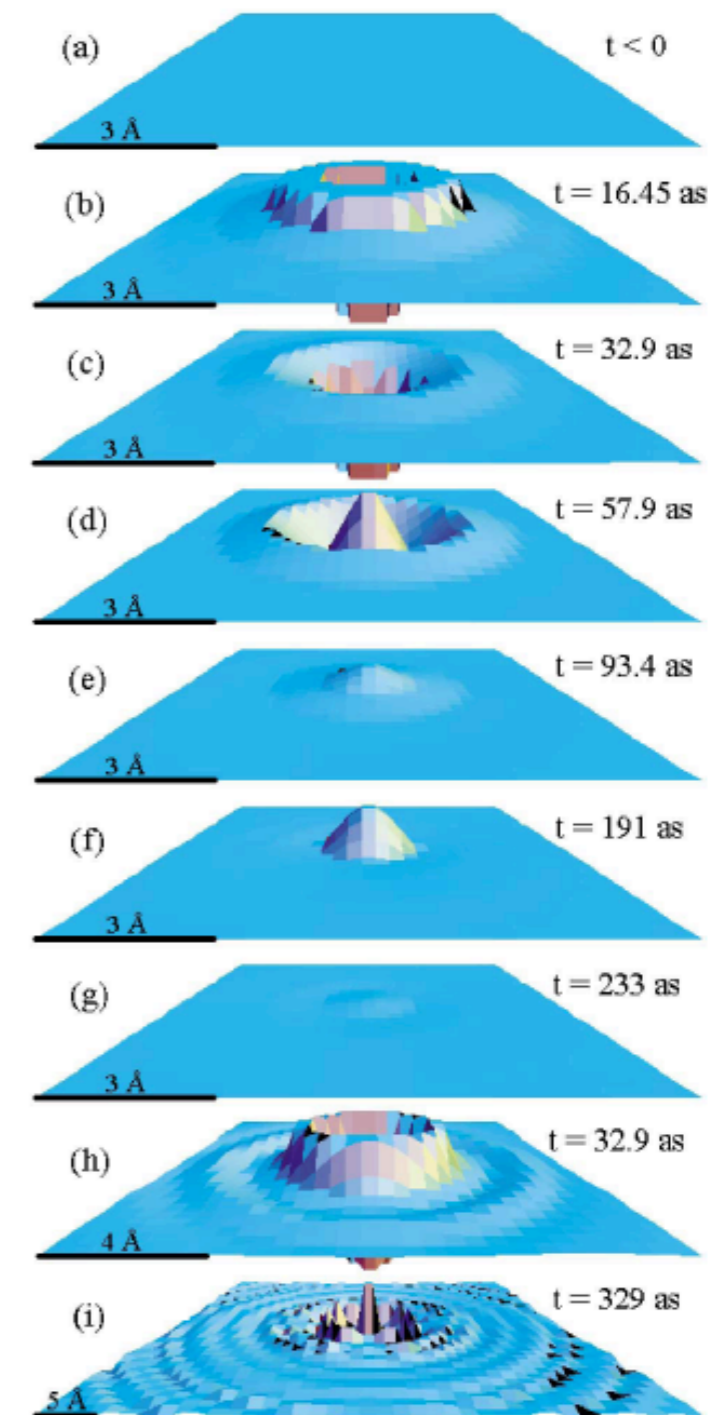
$$\text{Im } \chi(\mathbf{Q}, \omega)$$

↓ KKT

$$\text{Re } \chi(\mathbf{Q}, \omega)$$

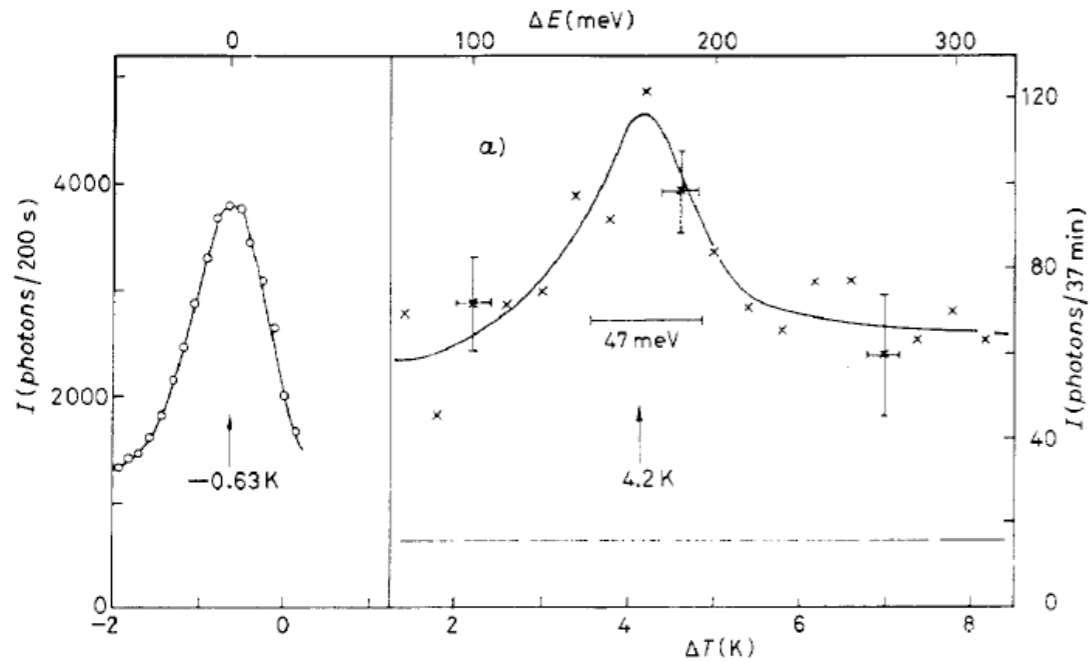
↓ FT

$$X(\mathbf{r}, t)$$



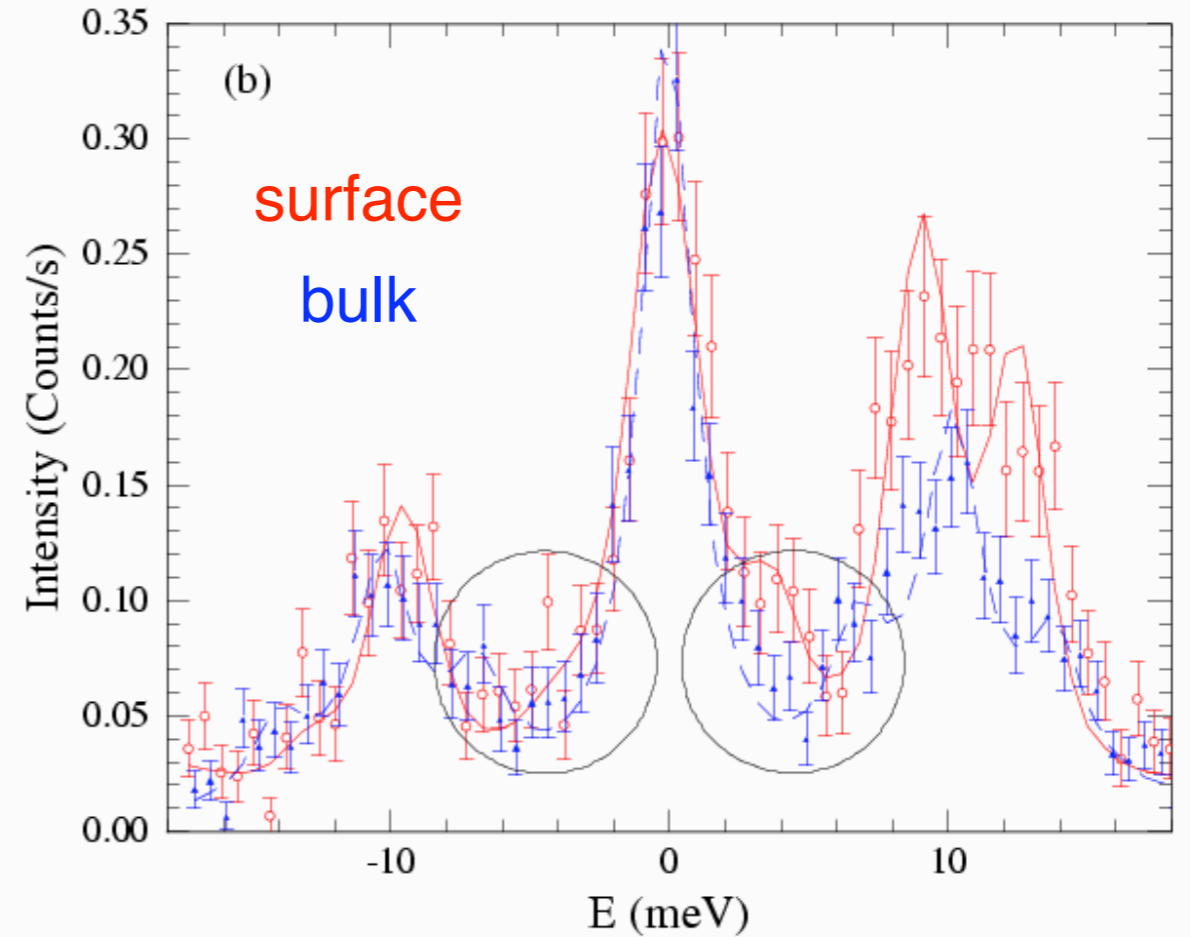
NIXS (phonon excitation)

1987 graphite (DORIS II, HASYLAB)



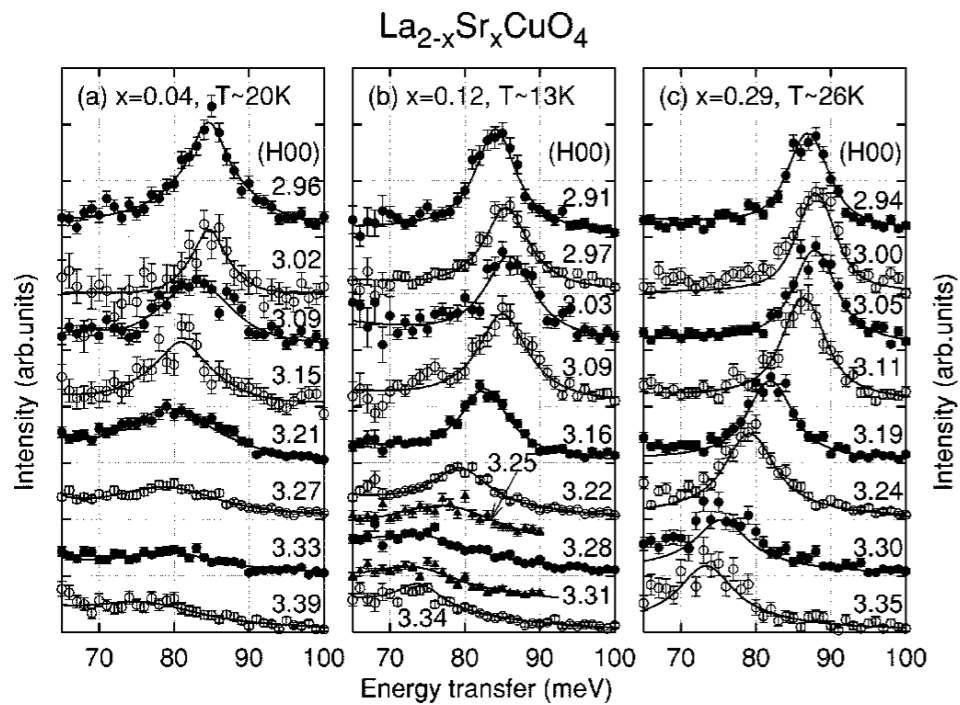
Burkel et al., EPL 3, 957 (1987)

2005 2H-NbSe₂ surface (ESRF)



Murphy et al., PRL 95, 256104 (2005)

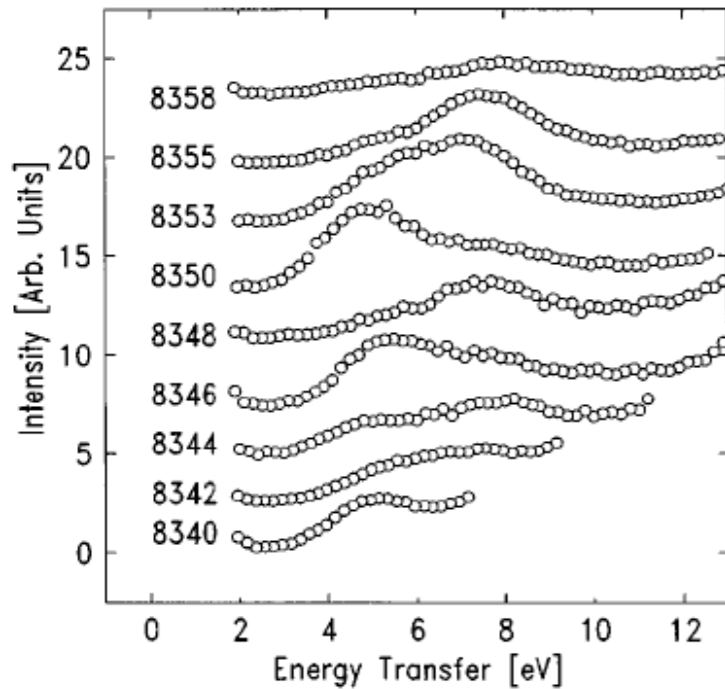
2005 La_{2-x}Sr_xCuO₄ (SPring-8)



Fukuda et al., PRB 71, 060501 (2005)

RIXS

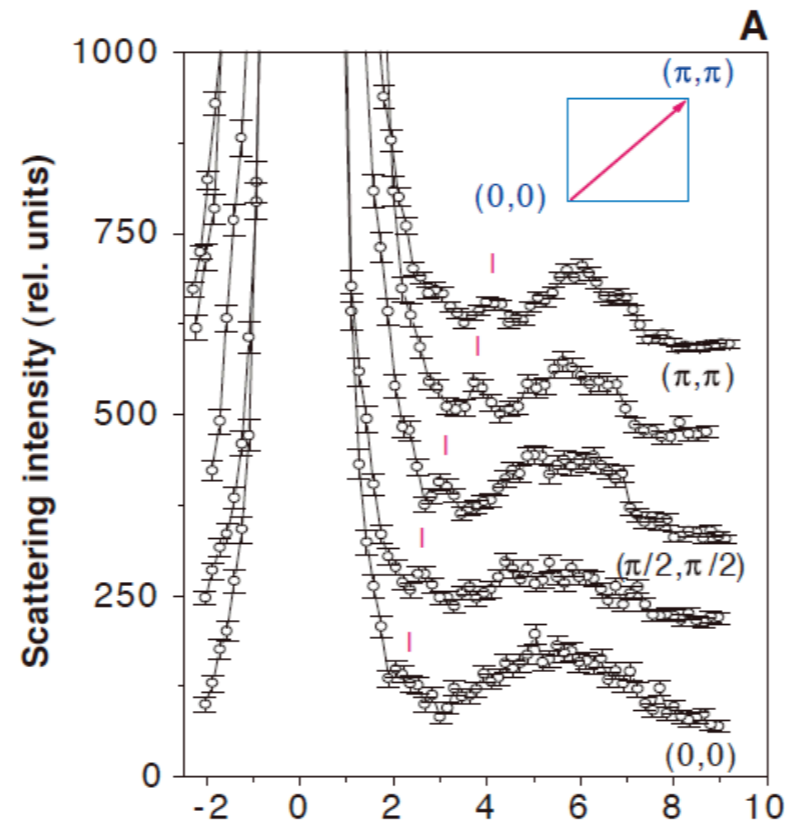
1996 $\omega = 6$ eV



NiO (CT gap)

Kao et al., PRB **54**, 16361 (1996)

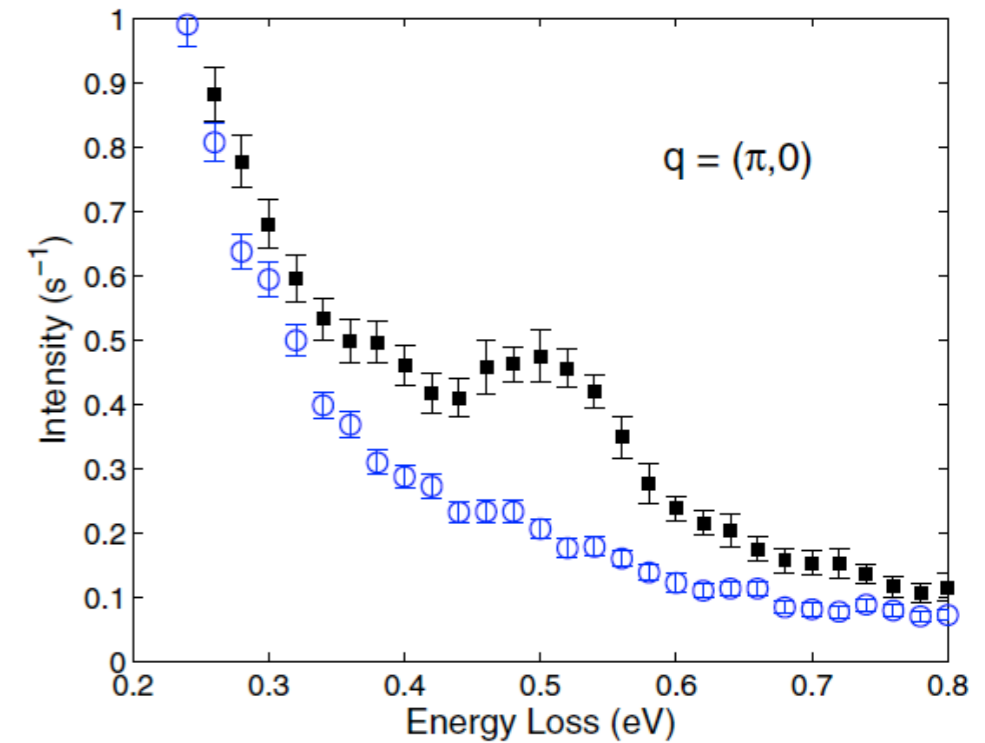
2000 $\omega = 2$ eV



$\text{Ca}_2\text{CuO}_2\text{Cl}_2$ (Mott gap)

Hasan et al., Science **288**, 1811 (2000)

2008 $\omega = 0.5$ eV



La_2CuO_4 (two magnon)

Hill et al., PRL **100**, 097001 (2008)

6 eV excitation in CuGeO_3

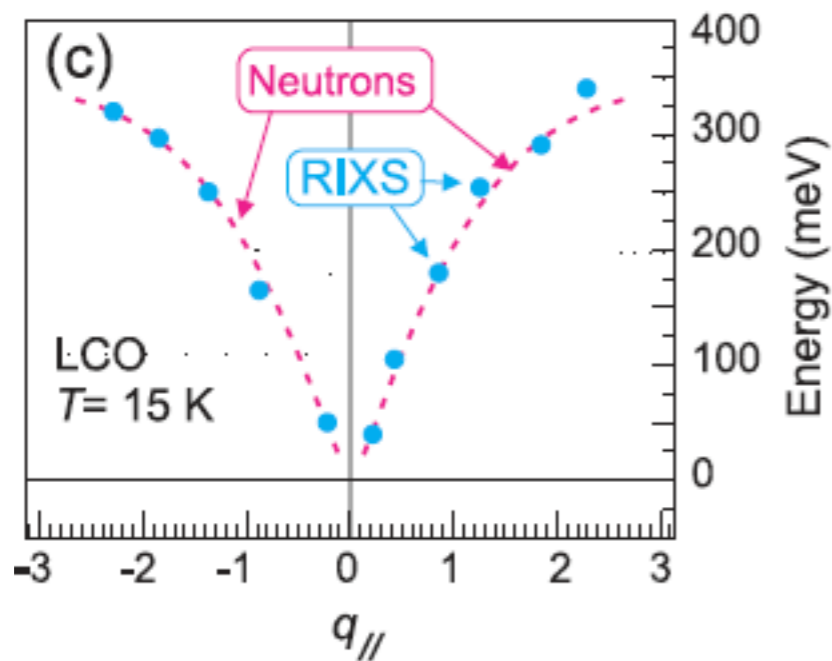
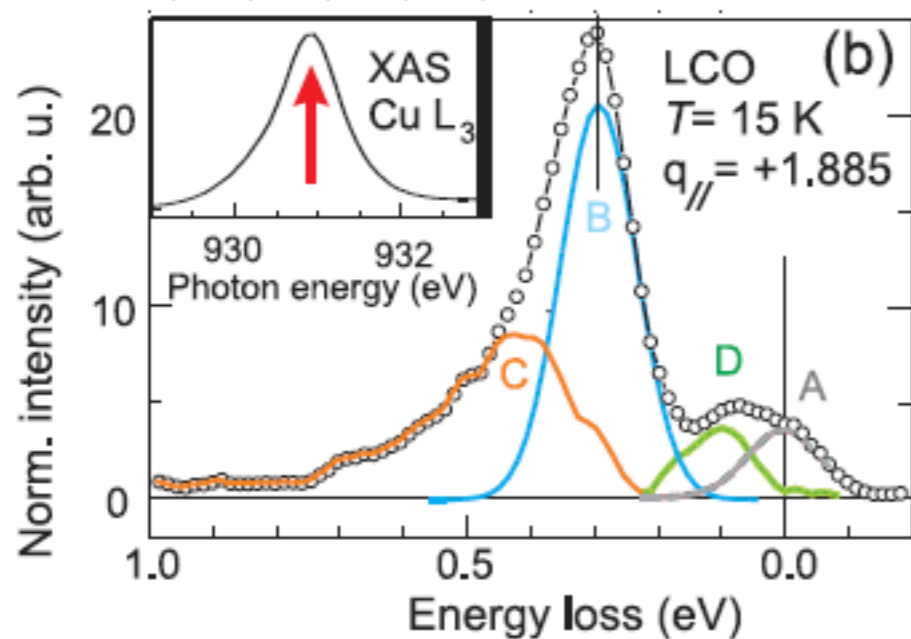
year	count rate (cps)	resolution (meV)	beamline	facility
1999	1	1500	X21	NSLS
2002	6	300	9IDB	APS
2006	50	115	30IDB	APS
2007	600	90	30IDB	APS

$I/\Delta E$ increased by 10^4 !

J. P. Hill's presentation at IMSS symposium'08

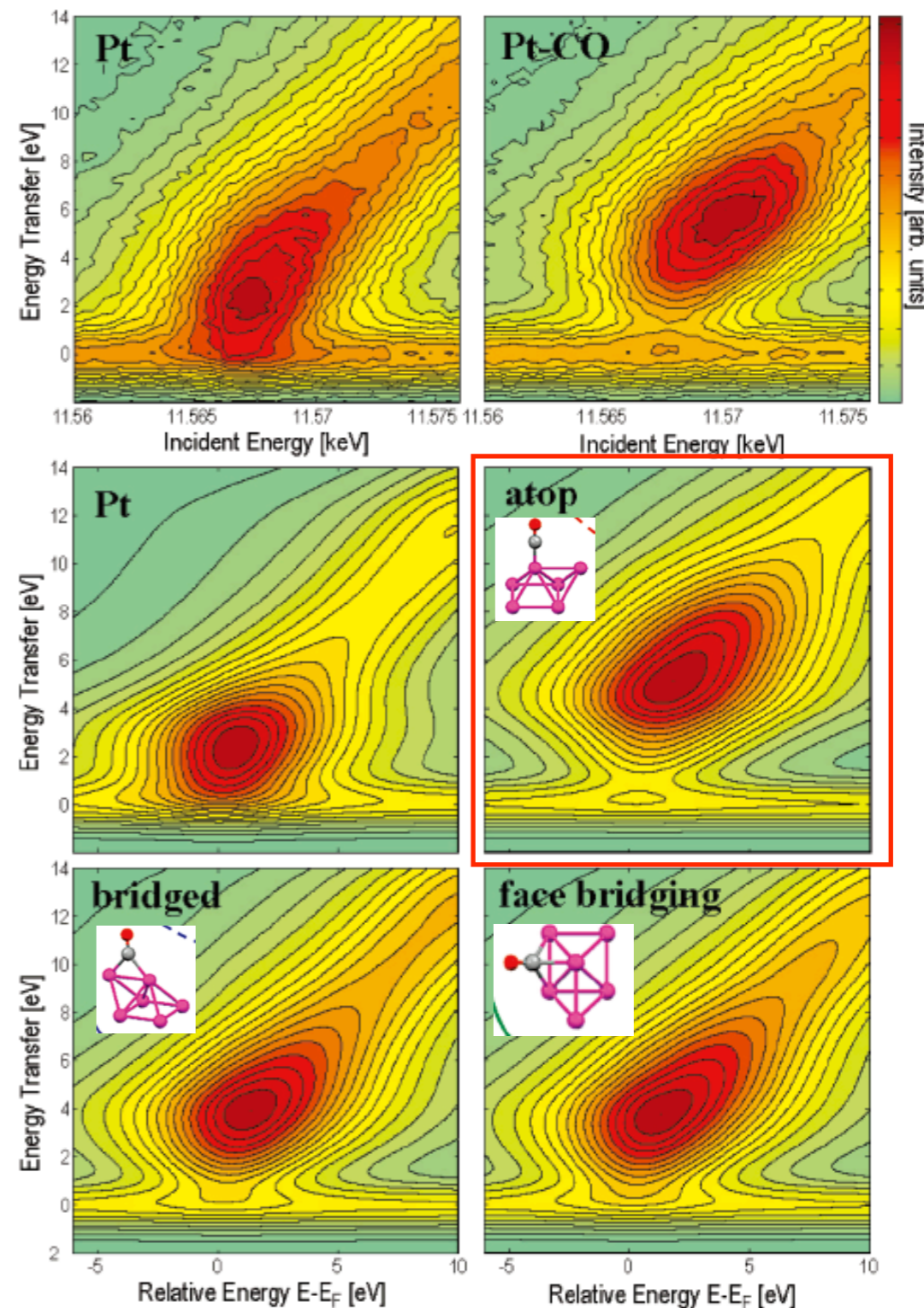
New direction of RIXS

Single magnon (spin wave)
[soft x-ray]



Braicovich et al., PRL **104**, 077002 (2010)

CO adsorbed Pt nano-particle
(in-situ, element-selective experiment)



Glatzel et al., JACS **132**, 2555 (2010) 12

Current x-ray sources for IXS

SPring-8



APS



ESRF



beamlines with insertion device at 3rd generation synchrotron facilities

	NIXS (phonon)	NIXS (electronic) RIXS
energy resolution	~ 1 meV	~ 100 meV
incident flux	10^9 photons/s/1meV [1]	10^{11} photons/s/100meV [2]
count rate	0.1 - 10 Hz	

Most experiments are flux-limited !

“photons/s/meV” is the key parameter for incident beam.

[1] BL35XU at SPring-8 : Baron et al., Nucl. Instrum. Methods Phys. Res. A **467-468**, 627 (2001)

[2] BL11XU at SPring-8 : Inami et al., Nucl. Instrum. Methods Phys. Res. A **467-468**, 1081 (2001)

XFELO

XFELO characteristics

KEK [<http://pfwww.kek.jp/adachis/erl/cn9/pg102.html>]

- Electron Beam Energy 7 GeV
- Bunch length 1 ps
- Emittance 0.2 mm-mrad
- Repetition rate 1 MHz
- Undulator 60 m
- X-ray energy range 5 - 25 keV
- Band width 10^{-7} (1 meV for 10 keV x-ray)
- photons/pulse 10^9

⇒ **10^{15} photons/s/meV !!**

Workshop of APS User Week 2010

- Photon energy coverage from 5 keV to 25 keV (and third harmonics)
- Tunable photon energy (5%)
- Fully coherent transversely and temporally
- High spectral purity with ~1 meV bandwidth
- Length of individual x-ray pulse ~ 0.1-1 ps
- Number of photons ~ 10^9 per pulse ($\sim 10^6 - 10^4$ for 3rd harmonics)
- Peak brightness comparable to that of SASE XFELs
- Pulse repetition rate ~1 MHz
- Time-averaged brightness is five orders of magnitude higher than that of the LCLS and three orders of magnitude higher than that of the European XFEL.

New era of IXS using XFEL

Improvement of incident flux by 6 orders of magnitude

→ NIXS for electronic excitations are really feasible.

- new electronic excitations at low energy (~ 1 meV)

- ◆ charge excitations

- phonon (excitation of all electrons in an atom) Intensity $\propto Z^2$

- electronic excitation of one electron Intensity $\propto 1^2$ (possible !)

- ◆ magnetic excitations

- $(\hbar\omega/mc^2)^2 \sim 10^{-6}$ of charge scattering (might be possible)

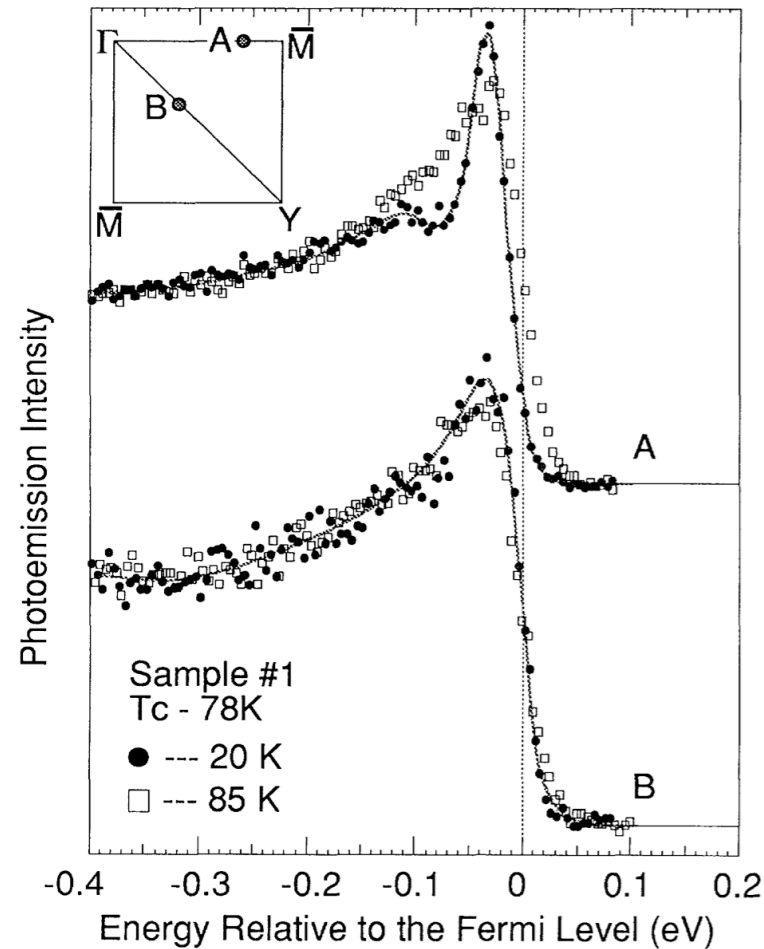
- truly complementary tool of inelastic neutron scattering

→ Extension of current techniques

- spatially- and/or temporally-resolved IXS (phonon, RIXS)
- extreme conditions

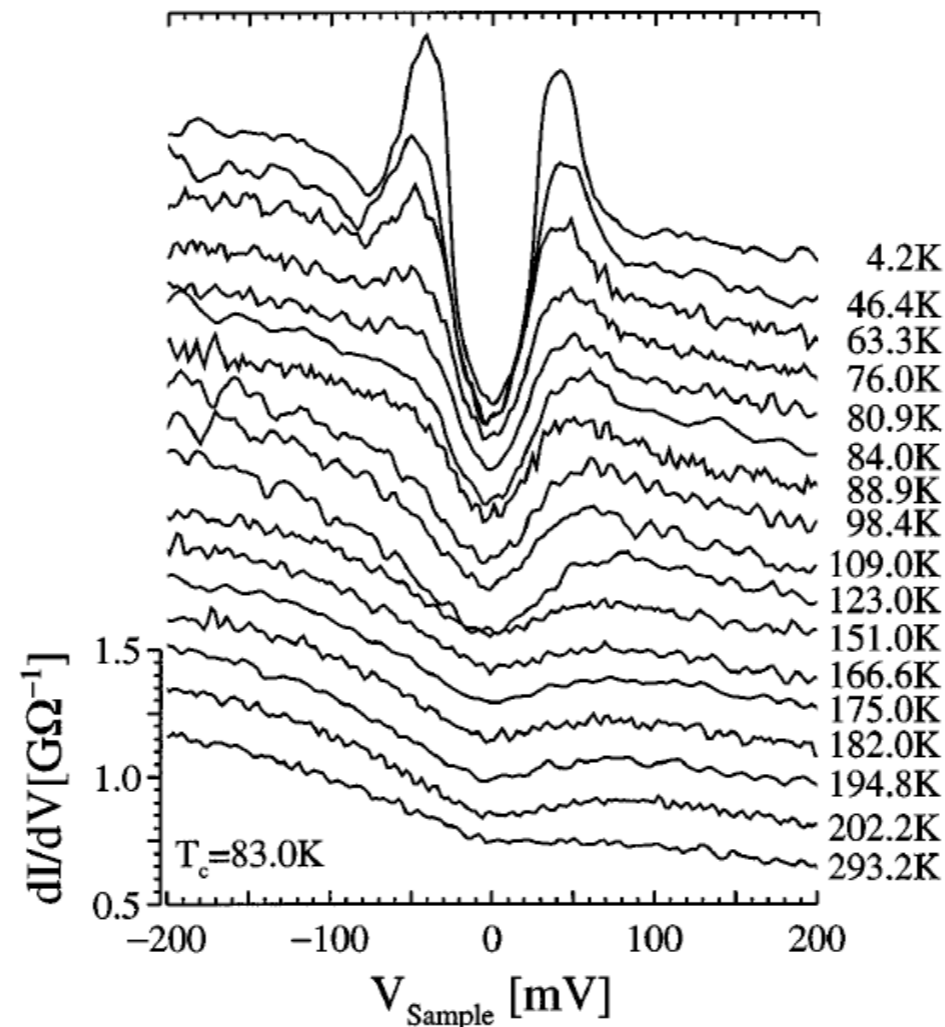
Superconducting gap

ARPES



Shen et al., PRL **70**, 1553 (1993)

STS



Renner et al., PRL **80**, 149 (1998)

SC gap (BCS theory)
 $\Delta_0 \sim 1.76k_B T_c$

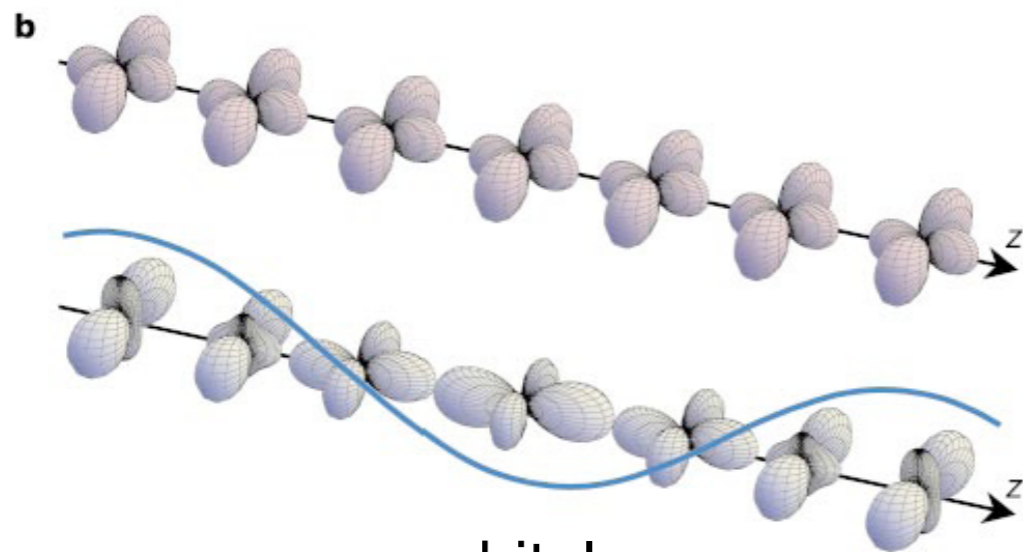
Gap in momentum space
↓
pairing symmetry

Both experimental techniques are powerful but surface sensitive.

Bulk sensitive measurement of SC gap by IXS could be available.

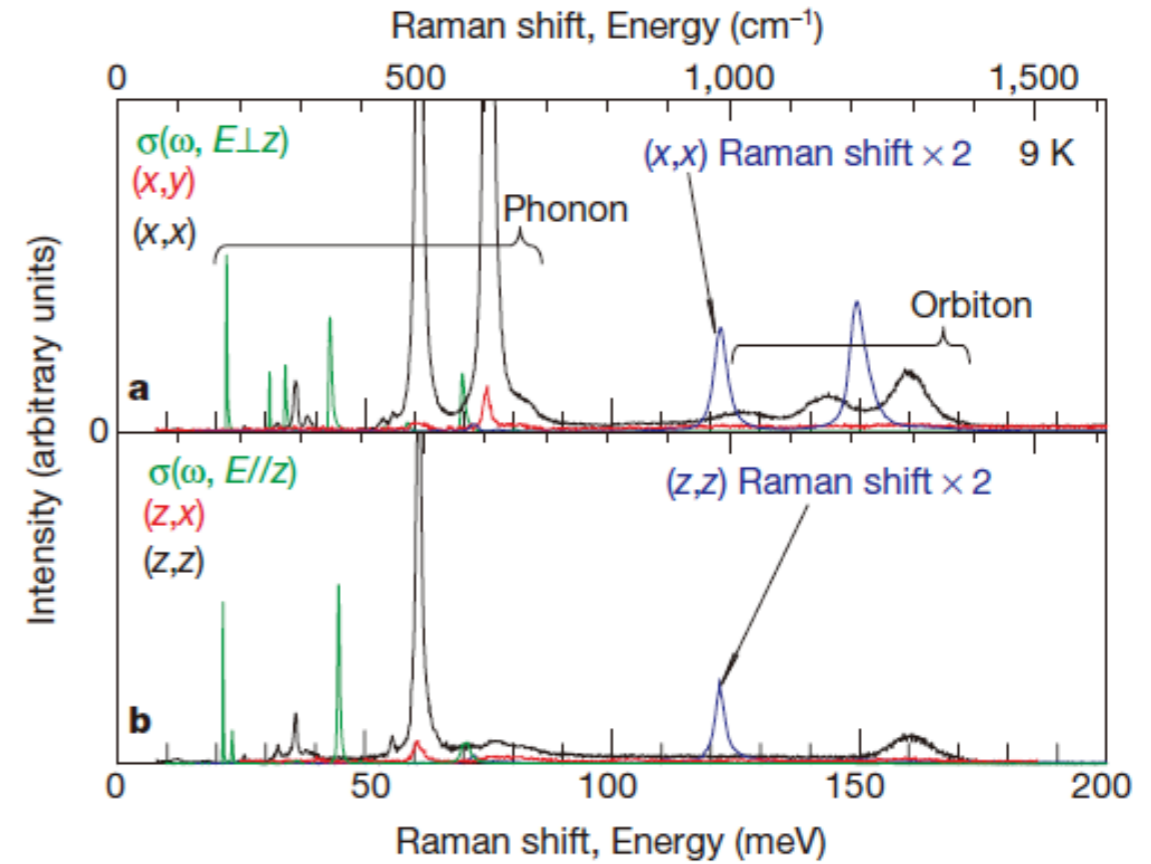
Collective orbital wave excitation (orbiton)

LaMnO₃

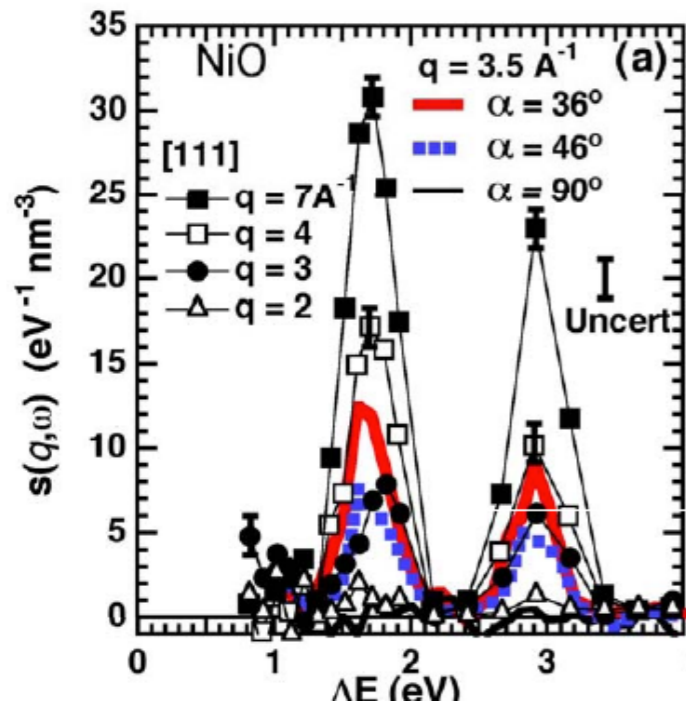


orbital wave

Saitoh et al., Nature **410**, 180 (2001).



By Raman scattering, orbiton was observed at $Q = 0$ but not at finite Q .



Dynamical structure factor

$$S(\mathbf{q}, \omega) = \sum_f |\langle \psi_f | e^{i\mathbf{q} \cdot \mathbf{r}} | \psi_i \rangle|^2 \delta(E_i - E_f + \hbar\omega)$$

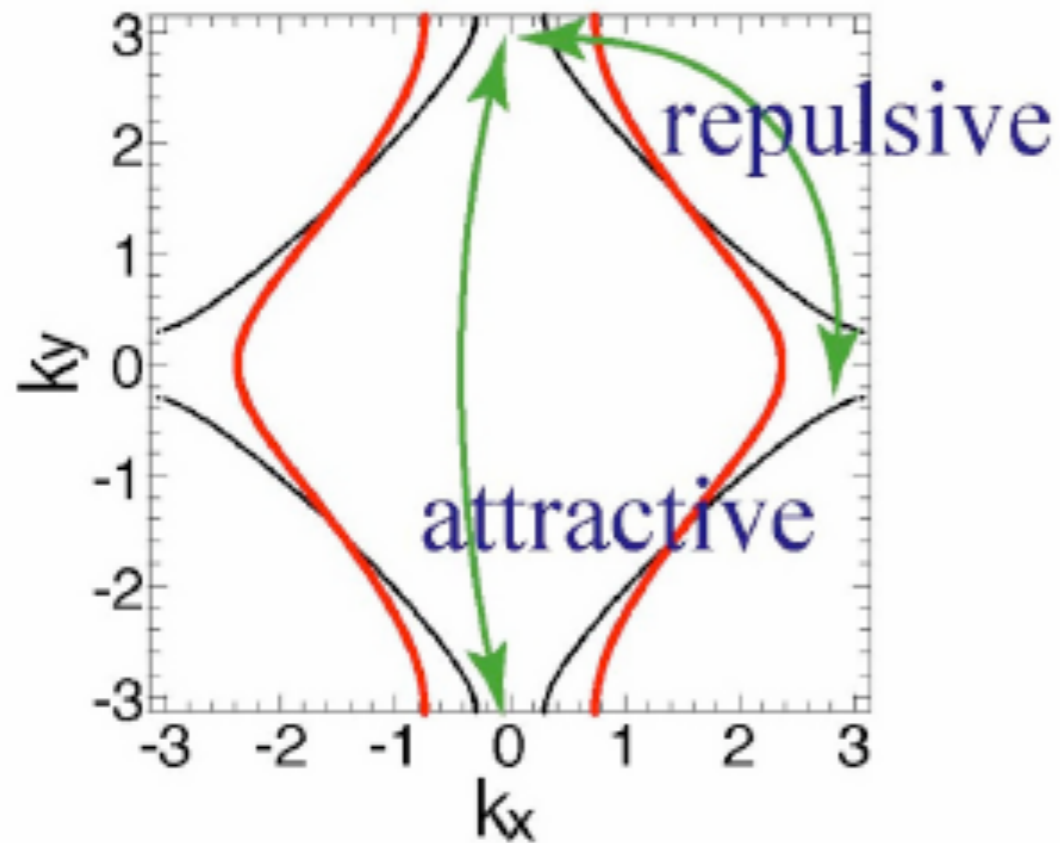
Non-dipole transition (e.g. d-d excitation) is possible at high Q of IXS.

Larson et al.,
PRL **99**, 026401 (2007).

d-wave Fermi surface deformation

H. Yamase (NIMS)

Spontaneous symmetry breaking of Fermi surface



t-J model

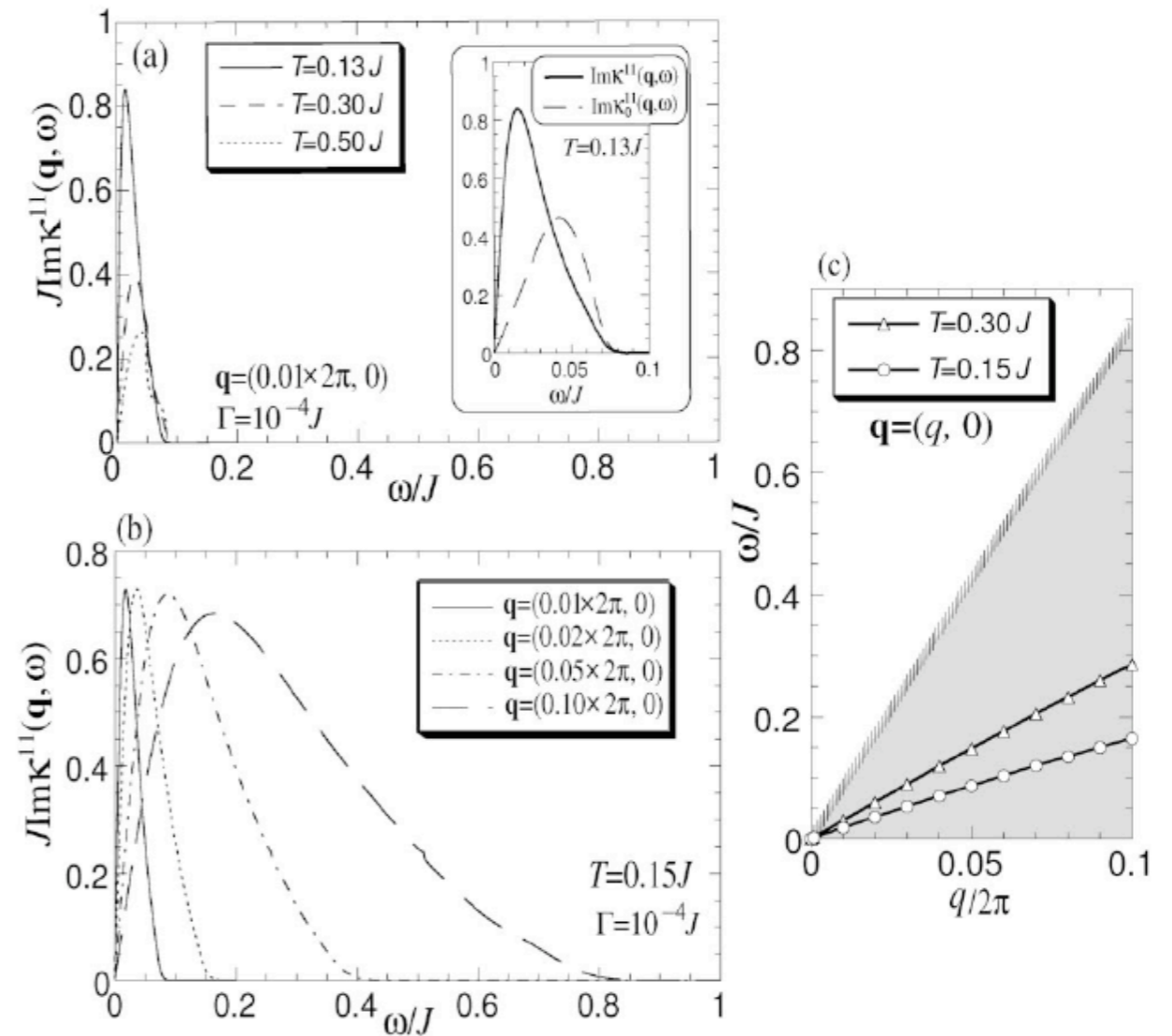
Yamase et al., JPSJ 69, 2151 (2000)

Hubbard model

Halboth et al. PRL 84, 5162 (2000)

d-wave Fermi surface deformation

d-wave Pomeranchuk instability



Yamase, PRL 93, 266404 (2004)

A dispersive excitation appears at $q \sim 0$.

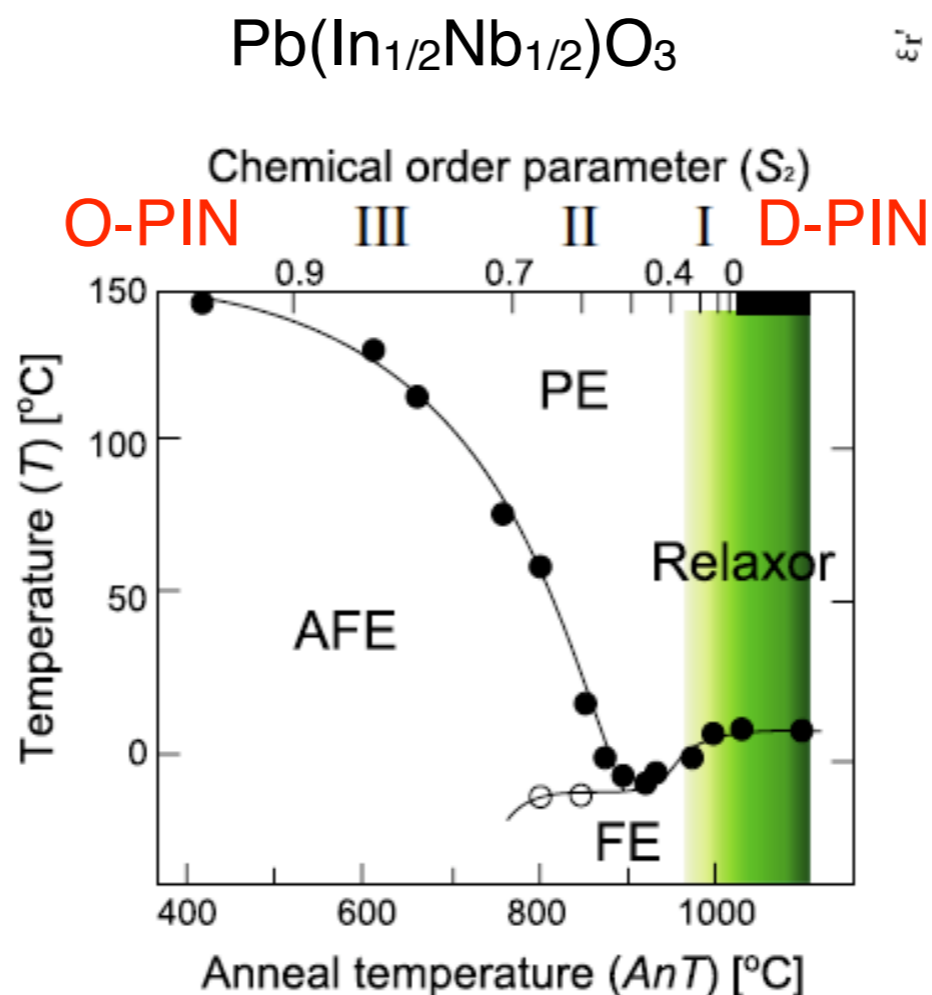
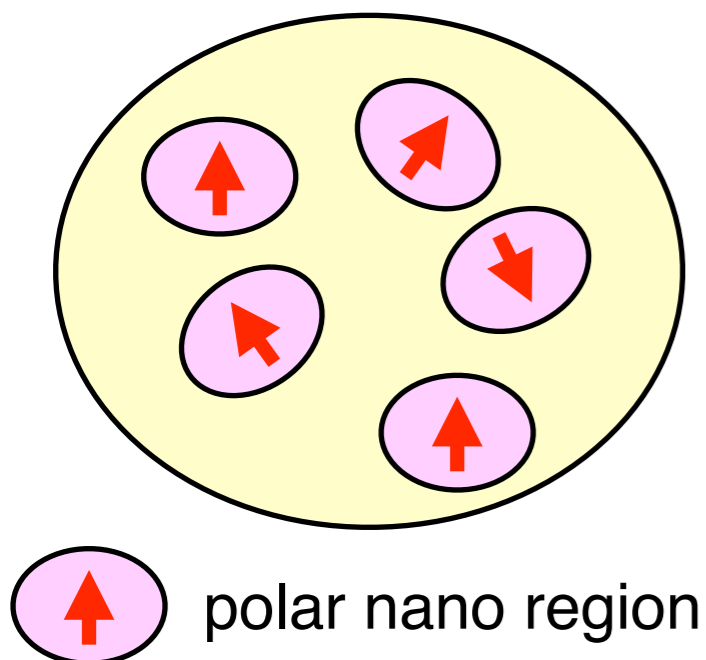
Spatially-resolved phonon measurement

K.Ohwada (JAEA)

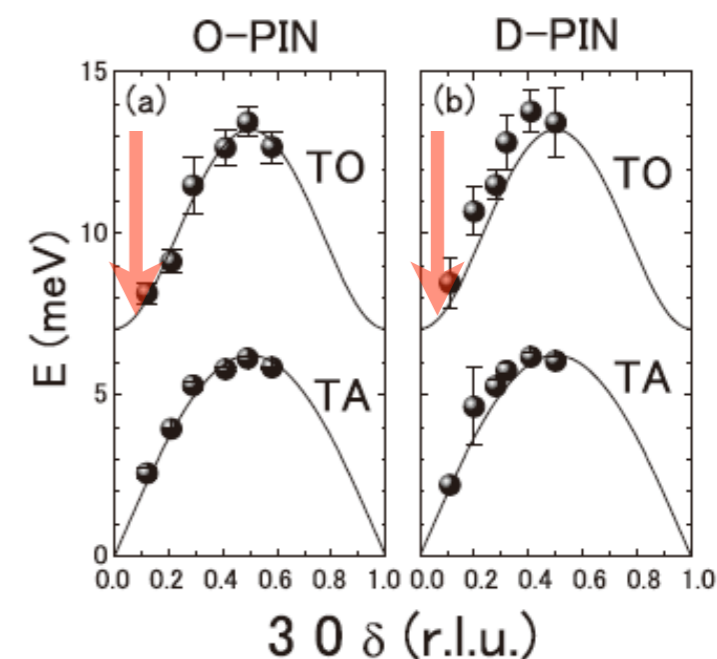
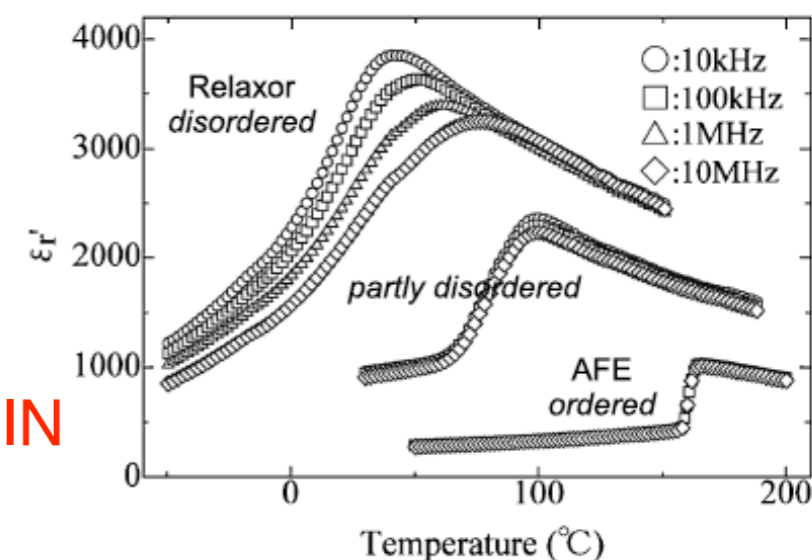
Inhomogeneity is often important for physical properties.

← Spatially-resolved experiment

relaxer



Ohwada et al., JPSJ 79. 011012 (2010)



FE fluctuation
in both O- and D-PIN

Spatially-resolved phonon measurement (hopefully nm scale)

→ Distinction of FE fluctuation between order and disorder regions (+ their boundary)
understanding of relaxer behavior

CO/NO catalytic reaction

successive exposure of CO and NO to Pd/Al₂O₃

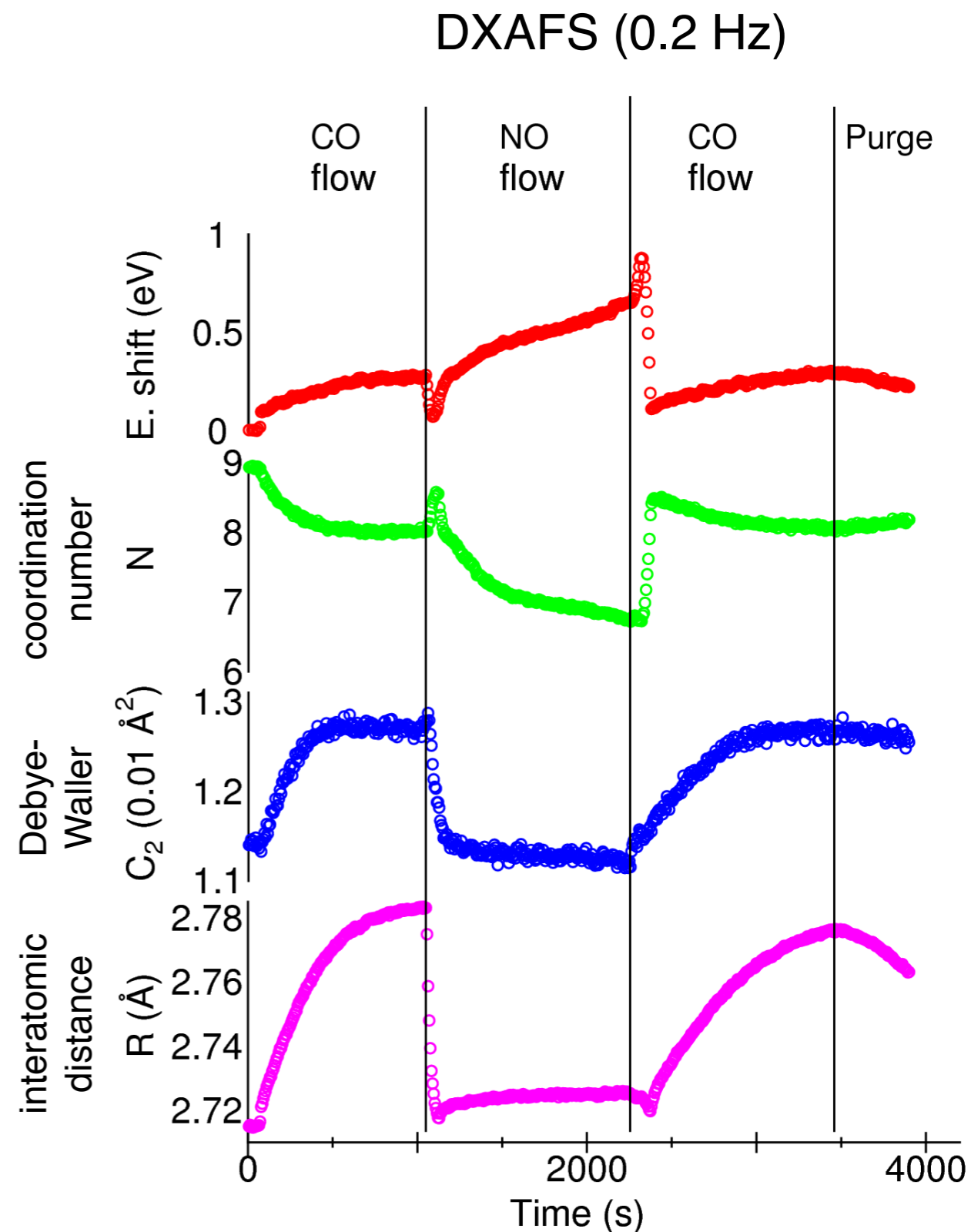
CO → CO₂ , NO → N₂

in-situ experiment ← x-ray spectroscopy

Temporally-resolved RIXS can give more detailed information on electronic states.

- identification of active d band
- distinction of adsorbed molecules

Understanding of catalytic reactions
based on electronic states



Summary

- Most of IXS experiments are flux-limited.
It will be overcome by x-rays from XFELs.

10^9 photons/s/meV \rightarrow 10^{15} photons/s/meV
improvement of incident flux by 6 orders of magnitude

Many new possibilities will open up!

- Proposed band width (~ 1 meV) is suitable for condensed matter physics
complementary use to real time approach

